Chinese Chemical Letters 37 (2026) 111254

Contents lists available at ScienceDirect

Chinese Chemical Letters

journal homepage: www.elsevier.com/locate/cclet

Diphtheria toxin-derived short peptide enables dual targeted delivery of vorinostat for glioma treatment

Tianheng Chen[a,1], Yanyu Zhang[b,1], Zhen Fang[a,1], Anze Liu[c], Yingxin Dong[c], Xiying Wu[d,*], Feng Yang[a,*], Huan Wang[c,e,*]

[a] Department of Inorganic Chemistry, School of Pharmacy, Naval Medical University, Shanghai 200433, China
[b] Institute of Analytical Technology and Smart Instruments, Xiamen Key Laboratory of Food and Drug Safety, College of Environment and Public Health, Xiamen Huaxia University, Xiamen 361024, China
[c] Department of Pharmaceutical Sciences, School of Pharmacy, Naval Medical University, Shanghai 200433, China
[d] Shanghai Skin Disease Hospital, Tongji University School of Medicine, Shanghai 200433, China
[e] The Center for Basic Research and Innovation of Medicine and Pharmacy (MOE), School of Pharmacy, Naval Medical University, Shanghai 200433, China

ARTICLE INFO

Article history:
Received 10 February 2025
Revised 20 April 2025
Accepted 22 April 2025
Available online 23 April 2025

Keywords:
Blood-brain barrier
Diphtheria toxin receptor
Glioma
Vorinostat
Peptide-drug conjugates

ABSTRACT

Glioma, a highly aggressive brain tumor with a dismal prognosis, faces significant treatment hurdles due to the blood-brain barrier, which limits the efficient delivery of most medications. Diphtheria toxin receptor (DTR) is a specific receptor expressed both on brain microvascular endothelial cells and glioma, emerging as a potentially valuable target for targeted drug delivery system for glioma treatment. In this work, a short peptide (designated DTX) derived from diphtheria toxin, was rational designed and chemical synthesized based on the binding domain to DTR. The function of DTX as a ligand of DTR and the brain/glioma dual targeting efficacy were evaluated *in vitro* and *in vivo*. Furthermore, DTX was conjugated to vorinostat (SAHA) to enable its anti-glioma efficacy. The results demonstrated that DTX-SAHA can effectively cross the blood-brain barrier, exhibiting promising anti-glioma efficacy with good biocompatibility. This research confirmed the potential of DTX as the ligand for DTR-mediated intracranial drug delivery.

© 2025 Published by Elsevier B.V. on behalf of Chinese Chemical Society and Institute of Materia Medica, Chinese Academy of Medical Sciences.

Gliomas rank among the most prevalent primary tumors of the central nervous system, notorious for the treatment difficulty, high recurrence rates and unfavorable prognosis [1,2]. Currently, the main clinical approaches for glioma treatment are centered around surgical resection, accompanied by radiotherapy and chemotherapy. Nevertheless, the blood-brain barrier (BBB) poses a significant physiological obstacle for the intracranial delivery of therapeutics [3]. Receptor-mediated transport (RMT) has emerged as one of the most effective non-invasive strategies for drug delivery across the BBB [4]. The specific receptors expressed on brain capillary endothelial cells (*e.g.*, transferrin receptor, nicotine acetylcholine receptor, and low-density lipoprotein receptor-related protein-1), possess the capability to recognize and facilitate the transport of respective ligands across the BBB [5,6].

Among these receptors, diphtheria toxin receptor (DTR), also referred to membrane-anchored heparin-binding epidermal growth factor (HB-EGF), stands out as an appealing target in RMT owing to its distinctive characteristics [7]. In contrast to transferrin receptor-mediated drug delivery, the absence of endogenous ligands for DTR mitigates the possibility of competitive interactions with these ligands [8]. Moreover, DTR is overexpressed not merely on brain capillary endothelial cells [9–12] but also on glioma cells [13,14], where its expression levels are positively correlated with the pathological grade of gliomas. This characteristic enables dual-targeted drug delivery, facilitating the simultaneous targeting of BBB and gliomas with a single ligand, thus streamlining targeting design strategies.

Diphtheria toxin (DT), the specific ligand for DTR, is secreted by *Corynebacterium diphtheria*. DT consists of two fragments, namely fragment A and B, which remain connected through a disulfide bridge. Fragment A encompasses the catalytic (C) domain, responsible for the toxicity of DT. Whereas fragment B contains the transmembrane (T) domain and C-terminal receptor-binding (R) domain [15,16]. DT binds to the EGF-like domain through its R-domain and is internalized into cells *via* clathrin-dependent receptor-mediated endocytosis [17]. The three domains of DT are functionally independent. To mitigate toxicity while preserving the ability to tar-

* Corresponding authors.
E-mail addresses: wxyifd@163.com (X. Wu), yangfeng1008@126.com (F. Yang), wang568855641@163.com (H. Wang).
[1] These authors contributed equally to this work.

https://doi.org/10.1016/j.cclet.2025.111254
1001-8417/© 2025 Published by Elsevier B.V. on behalf of Chinese Chemical Society and Institute of Materia Medica, Chinese Academy of Medical Sciences.

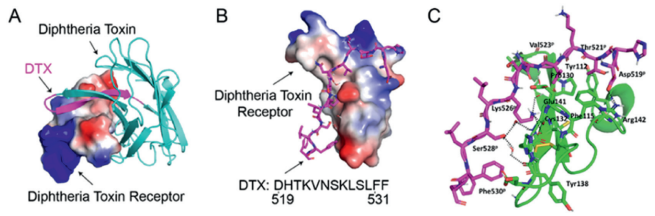


Fig. 1. Binding mode of DTX and diphtheria toxin receptor. (A) The diphtheria toxin receptor and diphtheria toxin. (B) DTX and diphtheria toxin receptor. Diphtheria toxin receptor was represented by electrostatic potential surface. The active peptides were shown in sticks and colored in purple. (C) The interaction details between DTX (purple) and diphtheria toxin receptor (green). The interacting residues were represented in sticks and the hydrogen bonds were shown by dash lines.

get BBB, researchers have developed various DT derivatives, including mutants and truncated forms of DT [18,19]. Some derivatives demonstrated promising potential in clinical and basic research include CRM107 [20], DT389-EGF [21], CRM197 [22,23], DTAT/DTAT13/DTATEGF [24,25], and DTEGF13 [26]. Nevertheless, these derivatives have certain drawbacks such as non-negligible toxicity, relatively large size or suboptimal binding affinity, which impeded their further application. Consequently, the identification of a non-toxic, short amino acid sequence from DT with sufficient affinity is of great significance for DTR-mediated intracranial drug delivery.

In this study, we delved into the structural intricacies of DT-DTR binding, uncovering a consecutive key sequence of 13 amino acids within the R-domain of DT that potentially engages with DTR. The synthetic peptide, DTX, corresponding to this region exhibits considerable binding affinity to DTR and can be effectively recognized by cells expressing DTR. Notably, the DTX facilitated the concurrent targeting of both the BBB and gliomas. Furthermore, vorinostat (SAHA), an inhibitor of histone deacetylase (HDAC), was conjugated with DTX to evaluate its anti-glioma potential. Our findings underscore the capacity of the DTX peptide has the ability to enable dual-targeted delivery of SAHA, which holds great promise for the efficient treatment of gliomas.

The binding affinity between the DT and DTR is relatively high, with an estimated apparent dissociation constant in the range of 10^{-8}–10^{-9} mol/L [27]. Despite both DT and DTR are relatively large in size, their binding hinges on a few crucial amino acids on the binding surface, which are arranged in the correct spatial orientation. The remaining amino acids of the protein function more as a scaffold, providing structural stability. Consequently, it is feasible to identify a small segment of amino acids on the binding surface of a DT-DTR that is sufficient for the association. DT is composed of three distinct structural domains: C domain (residues 1–188), T domain (residues 200–378) and R domain (residues 387–535). The chemical structure of DT revealed that it can specifically bind to DTR through face-to-face interaction of β-sheets in R domain [28,29]. As reported by Rolf *et al.* [30], a peptide extracted from the C-terminal of the R domain of DT (residues 482–535) was shown to inhibit competitively binding of toxin to the receptor. This suggested that only the part of the C-terminal of the R domain of DT is required for DTR binding. Additionally, truncation of the residues after K526 completely abolishes binding. Based on these findings, we extracted the residues 519–531 of DT to design a new peptide DTX (sequence: DHTKVNSKLSLFF) with a relatively simple structure yet considerable DTR binding affinity. A molecular docking study was performed to explore the interaction between DTX and DTR as illustrated in Figs. 1A and B. Lys526^{P} formed a hydrogen-bond network with the carbonyl oxygens of DTR-Cys132 and Glu141, along with a water molecule. Asp519 formed ionic interaction with Arg142. Ser528^{P} formed a hydrogen bond network with two water molecules and the carbonyl oxygen of Tyr138. All these hydrogen bond interactions were also present in the crystal structure of the DT-DTR complex. The sidechains of Val523^{P} and Thr521^{P} stretched into the hydrophobic pocket formed by Pro130, Tyr112 and Phe130 (Fig. 1C).

DTX was chemically synthesized according to the designed amino acid sequence in this critical region. A cysteine was introduced at its N-terminus to facilitate subsequent chemical modification of DTX. As depicted in Fig. S1 (Supporting information), DTX was prepared using Fmoc-based solid-phase peptide synthesis. After purification and lyophilization, DTX was obtained as a pure white powder. The purity of the DTX peptide was examined using high performance liquid chromatography (HPLC). The highest peak value was detected at a retention time of 8.16 min, with a purity exceeding 98 % (Fig. S2 in Supporting information). Electro spray ionization-mass spectroscopy (ESI-MS) revealed that the molecular weight of the peptide DTX corresponded to the estimated theoretical molecular weight of 1638.91, as shown in Fig. S3 (Supporting information). These results established the successful synthesis of the DTX peptide.

To track the cellular uptake, the fluorescent dye FAM was covalently linked to DTX. As shown in Figs. S4A and B (Supporting information), DTX was effectively uptaken by human brain microvascular endothelial cells (hBMEC) and U87 cells with flow cytometry analysis. The enhanced cellular uptaken of DTX was attributed to the DTR, which could be recognized by DTX to facilitate the uptake (Fig. S4C in Supporting information). Pretreating cells with anti-HB-EGF (a DTR antibody) significantly reduced DTX uptake, further confirming this mechanism. As shown in Figs. 2A and B, confocal microscopy images directly visualized DTX's cellular binding and its strong colocalization with DTR. To evaluate the *in vitro* trans-BBB transport capability of DTX, the BBB model was successfully established with the hBMEC trans-endothelial electrical resistance (TEER) value over 250 Ω cm^2 (Fig. S5A in Supporting information). The fluorescence intensity of solutions retrieved from the lower compartment in the DTX-FAM group exhibited a marked elevation compared to free FAM at various time intervals (Fig. S5B in Supporting information). Specifically, the transport rate of DTX-FAM was approximately twice that of FAM at 3 h, suggesting effective RMT process by DTX and DTR. The lower compartment was additionally seeded with U87 cells for further glioma targeting. As evidenced in Figs. S5C and D (Supporting information), the DTX-FAM was efficiently internalized by U87 cells located in the lower chamber. To investigate the *in vivo* BBB targeting ability of DTX, the fluorescent dye Cy5 was covalently linked to DTX and injected i.v. into the normal mice (all animal experiments were carried out in accordance with guidelines evaluated and approved by the Ethics Committee of Naval Medical University). Thirty minutes post-injection, a significant distribution of the fluorescein was observed in the brains of mice treated with DTX-Cy5, as presented in Figs. 2C and D and Fig. S6 (Supporting information). Upon further slicing of the brains, fluorescein imaging demonstrated a prominent accumulation of DTX-Cy5 within the brain tissue, which colocalized well with blood vessels (Fig. 2E). To investigate the *in vivo* glioma targeting ability of DTX, the intracranial U87 xenograft orthotropic model was established. Significant distribution of DTX-Cy5 within the glioma zone was also observed 1 h after intravenous administration (Fig. 2F). Fluorescence images of the tumor sections further revealed that DTX-Cy5 was leaking out of the brain vessels and being taken up by glioma cells (Fig. 2G). Collectively, the above results indicated that DTX possessed a dual-targeting ability towards both the BBB and glioma.

SAHA, an HDAC inhibitor, exerts effects by altering gene expression, thereby inducing growth arrest or apoptosis in tumor cell [31,32]. SAHA has demonstrated anti-proliferative effects on a variety of tumor cell types. Nevertheless, its therapeutic effect against

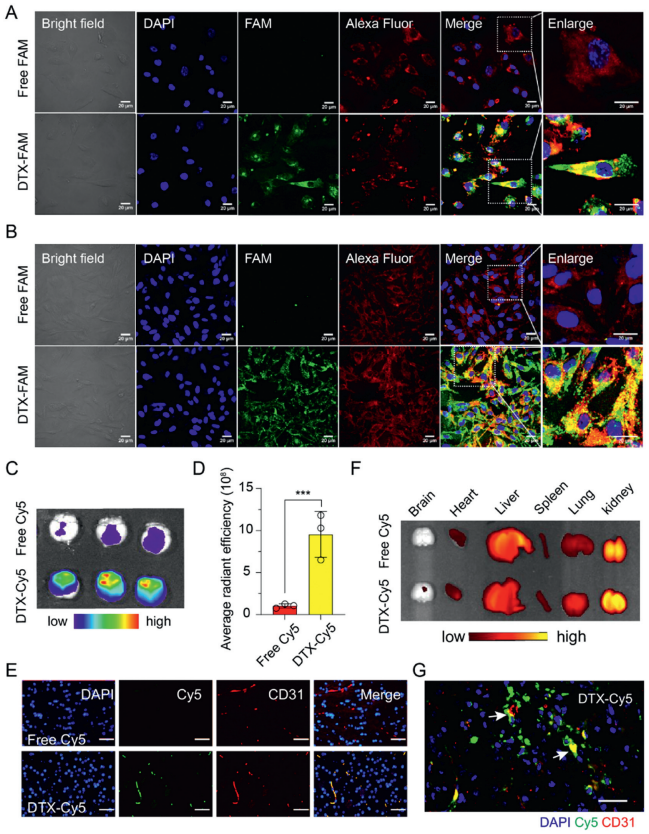


Fig. 2. Dual-targeting ability of DTX to the BBB and glioma. Confocal microscopy images of cellular uptake of DTX in hBMEC (A) and U87 cells (B). Blue represents the cell nuclei stained with 4′,6-diamidino-2-phenylindole (DAPI), green denotes DTX-FAM or free FAM, red signifies DTR labeled with a fluorescent secondary antibody, and yellow indicates the overlapping color resulting from the colocalization of DTX with DTR. Scale bar: 20 μm. *Ex vivo* fluorescence images (C) and semi-quantitative analysis (D) of brain tissues from normal BALB/c mice 30 min post-injection of free Cy5 and DTX-Cy5 ($n = 3$). (E) Fluorescence images of the brain slices after administration of free Cy5 and DTX-Cy5. (F) *Ex vivo* fluorescence images of the main organs from glioma-bearing BALB/c nude mice 1 h post-injection of free Cy5 and DTX-Cy5 ($n = 3$). (G) Fluorescence image of the glioma slices from glioma-bearing BALB/c nude mice 1 h post-injection of DTX-Cy5. In Figs. 2E and G, blue represents the cell nuclei stained with DAPI, green denotes DTX-Cy5 or free Cy5, red signifies blood vessels labeled with CD31 antibody, and yellow indicates the overlapping color resulting from red with green. The white arrow indicated DTX-Cy5 leaking out of the brain vessels. Scale bar: 50 μm. Data are means ± SD. $^{***}P < 0.001$.

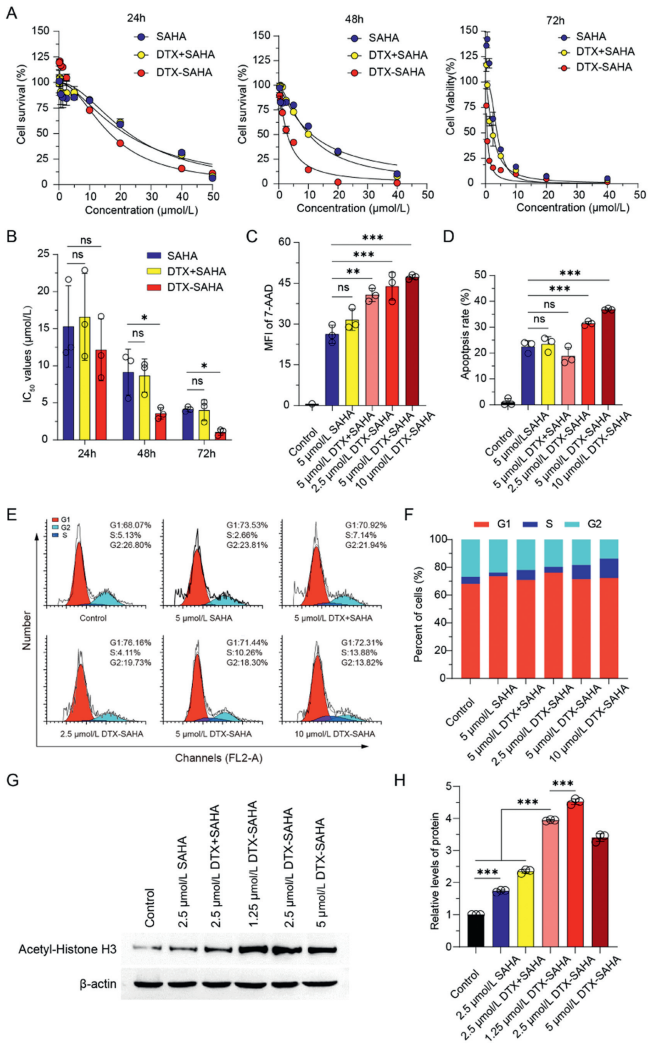


Fig. 3. Cytotoxicity of DTX-SAHA against U87 cells. (A) Cell viability after treatments with different concentrations of SAHA, DTX+SAHA and DTX-SAHA for 24, 48, and 72 h, respectively. (B) IC_{50} values calculating from the viability curves. (C) Cell viability stained with 7-AAD after treatments with SAHA, DTX+SAHA or DTX-SAHA for 24 h. (D) Cell apoptosis after treatments with SAHA, DTX+SAHA or DTX-SAHA for 24 h. (E, F) Cell cycle and statistical analysis of the percentage of cells in different arrest phases after treatments with SAHA, DTX+SAHA or DTX-SAHA for 24 h. Western blot assay (G) and semi-quantitative analysis (H) of the expression of acetyl-histone H3 in U87 cells. Data are means ± SD ($n = 3$). ns: no significant difference. $^{*}P < 0.05$, $^{**}P < 0.01$, $^{***}P < 0.001$.

glioma is hindered by the BBB. Consequently, DTX was conjugated to SAHA to develop the peptide-drug conjugate (DTX-SAHA). DTX-SAHA was obtained by conjugating the SAHA to the carboxylic acid terminus of DTX peptide *via* Fmoc-based solid-phase synthesis (Fig. S7 in Supporting information). The successful synthesis of DTX-SAHA was confirmed *via* characterization of HPLC, ESI-MS and nuclear magnetic resonance spectroscopy (^{1}H-NMR) spectrum, as depicted in detail in Figs. S8–S13 (Supporting information).

The cytotoxicity of DTX-SAHA against U87 cells was assessed *via* cell counting kit-8 (CCK-8) assay. As shown in Figs. 3A and B, DTX-SAHA exhibited enhanced cytotoxicity against U87 cells when compared to free SAHA and a mixture of DTX and SAHA (DTX+SAHA). This cytotoxic advantage became more pronounced as the treatment duration lengthened. Specially, the half maximal inhibitory concentration (IC_{50}) value for DTX-SAHA during 24 h of treatment (12.15 μmol/L) surpassed that of both SAHA (15.30 μmol/L) and DTX+SAHA (16.58 μmol/L). Upon extending the treatment duration to 48 and 72 h, the IC_{50} values for DTX-SAHA further declined to 3.58 and 1.06 μmol/L, respectively, significantly lower than SAHA (9.14 μmol/L at 48 h; 4.13 μmol/L at 72 h) and DTX+SAHA (8.67 μmol/L at 48 h; 4.02 μmol/L at 72 h), with statistical significance. Cytotoxicity assessment using 7-aminoactinomycin D (7-AAD) staining yielded consistent results (Fig. 3C). DTX-SAHA induced apoptosis of U87 cells in a concentration-dependent manner as evidenced in Fig. 3D U87 cells treated with DTX-SAHA underwent cell cycle arrest at the G1/S phase, and the number of cells in the G2 phase decreased in a gradient with increasing drug concentrations (Figs. 3E and F). The expression of acetyl-histone H3 in U87 cells was investigated using Western blot and the results are shown in Figs. 3G and H. DTX-SAHA potently enhanced histone H3 acetylation of U87 cells in a concentration-dependent manner, distinguishing it from other treatments.

The survival curves of the BALB/c nude mice bearing intracranial U87 xenograft treated with saline, SAHA, DTX+SAHA and DTX-SAHA were presented in Fig. 4A. DTX-SAHA was able to effectively extend the median survival time of the model mice to 38 days, significantly outperforming the other groups. Representative whole-brain hematoxylin-eosin (H&E) staining images, as depicted

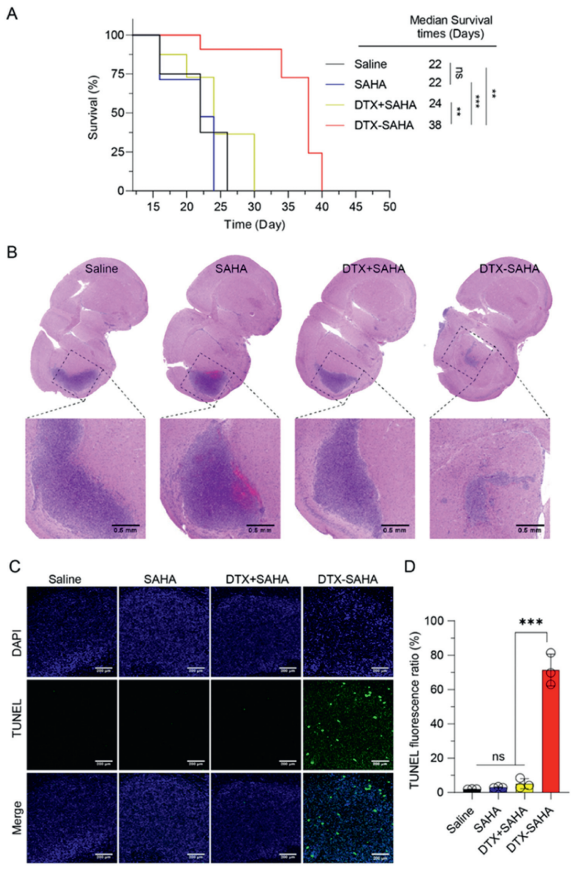


Fig. 4. Anti-glioma effect of DTX-SAHA *in vivo*. (A) Survival curves of BALB/c nude mice bearing intracranial U87 glioblastoma ($n = 8$). Mice were injected i.v. at 6, 8, 10, 12 and 14 days after glioma implantation with saline SAHA (20 mg/kg), DTX+SAHA (20 mg/kg), and DTX-SAHA (20 mg/kg). (B) Whole-brain HE staining section scan images of BALB/c nude mice from each group with dark areas indicating glioma lesions. (C) Immunohistochemical staining images of glioma tissue slices from BALB/c nude mice in each treatment group. DAPI: blue; TUNEL: green. Scale bar: 20 μm. (D) Statistical analysis of TUNEL staining fluorescence intensity in each group. Means ± SD ($n = 3$). ns: no significant difference. $^{**}P < 0.01$, $^{***}P < 0.001$.

in Fig. 4B, demonstrated that DTX-SAHA effectively suppressed glioma growth, exhibiting the smallest tumor lesions among all the treatment groups. Immunohistochemical staining analysis was conducted on the glioma tissues of the mice post-treatment as shown in Figs. 4C and D. The DTX-SAHA group exhibited the highest fluorescence intensity in terminal deoxynucleotidyl transferase-mediated dUTP-biotin nick end labeling (TUNEL) staining, indicating the most substantial level of tumor apoptosis. Overall, the results highlight the potent ability of DTX to potentiate the anti-glioma effect of SAHA.

Furthermore, upon completion of the final administration, the mice were sacrificed, and all organs were sampled for H&E staining as presented in Fig. S14A (Supporting information). Examination revealed that the lungs from the SAHA and DTX+SAHA groups exhibited multiple areas of alveolar wall capillary congestion (indicated by black arrows). In contrast, the lungs of the DTX-SAHA group did not exhibit any discernible damage. Moreover, no significant damage was observed in other organs of the mice treated with DTX-SAHA. All the blood routine parameters and biochemical indexes of mice treated with DTX-SAHA remained within the normal range after administration (Figs. S14B and C in Supporting information). Additionally, there were also no significant fluctuations in body weight or body temperature of the mice of the DTX-SAHA group during the treatment period as shown in Fig. S15 (Supporting information). Collectively, these findings established the good safety profile of DTX-SAHA administration.

In this study, based on the key amino acids at the binding surface, a short peptide ligand of DTR was developed, namely DTX. The synthesized DTX peptide demonstrates remarkable binding affinity to DTR and can be effectively recognized by cells that express DTR. As a result, the DTX peptide possesses the ability to traverse the BBB and actively target glioma. Both *in vitro* and *in vivo* studies validated the potential of DTX-conjugation in improving therapeutic efficacy of existing anticancer drugs, like SAHA, in the treatment of glioma. Given the encouraging results of DTX in brain/glioma-targeted drug delivery, this research laid the groundwork for DTR-mediated intracranial drug delivery for the treatment of central nervous system diseases.

Declaration of competing interest

The authors declare that they have no known competing financial interests or personal relationships that could have appeared to influence the work reported in this paper.

CRediT authorship contribution statement

Tianheng Chen: Writing – original draft, Methodology, Investigation. **Yanyu Zhang:** Writing – original draft, Methodology, Investigation, Funding acquisition. **Zhen Fang:** Writing – original draft, Methodology, Investigation. **Anze Liu:** Investigation, Formal analysis. **Yingxin Dong:** Investigation, Formal analysis. **Xiying Wu:** Writing – review & editing, Supervision, Investigation, Funding acquisition, Conceptualization. **Feng Yang:** Writing – review & editing, Validation, Supervision, Funding acquisition, Conceptualization. **Huan Wang:** Writing – review & editing, Supervision, Investigation, Funding acquisition, Data curation, Conceptualization.

Acknowledgments

This work was supported by the National Natural Science Foundation of China (Nos. 82373817 and 82473891), Basic Medicine School of Naval Medical University (No. JCKFKT-ZD-001), Shanghai Sailing Program (No. 23YF1457600), Natural Science Foundation of Fujian Province, China (No. 2023J011668), Natural Science Foundation of Xiamen, China (No. 3502Z20227083), Fujian Provincial Department of Education Young and Middle-aged Teachers Education Research Project, China (No. JAT210591).

Supplementary materials

Supplementary material associated with this article can be found, in the online version, at doi:10.1016/j.cclet.2025.111254.

References

[1] Y. Liu, W. Wang, D. Zhang, et al., Exploration 2 (2022) 20210274.
[2] Y. Xing, F. Yasinjan, M. Yang, et al., Nano Today 52 (2023) 101961.
[3] B. Feng, X. Lu, G. Zhang, L. Zhao, D. Mei, Acta Materia Medica 2 (2023) 216–227.
[4] J. Gao, Z. Xia, S. Gunasekar, et al., Nat. Rev. Mater. 9 (2024) 567–588.
[5] Z. Xie, G. Zhang, Y. Meng, et al., Chin. Chem. Lett. 35 (2024) 109584.
[6] Z. Zhang, J. Guan, Z. Jiang, et al., Nat. Commun. 10 (2019) 3561.
[7] A. Antignani, E.C.H. Ho, M.T. Bilotta, et al., Biomolecule 10 (2020) 1331.
[8] J. Rip, G.J. Schenk, A.G. De Boer, Expert Opin. Drug Deliv. 6 (2009) 227–237.
[9] P.J. Gaillard, A. Brink, A.G. de Boer, Int. Congr. Ser. 1277 (2005) 185–198.
[10] K. Mishima, S. Higashiyama, Y. Nagashima, et al., Neurosci. Lett. 213 (1996) 153–156.
[11] T. Nakagawa, M. Sasahara, Y. Hayase, et al., Dev. Brain Res. 108 (1998) 263–272.
[12] N. Tanaka, M. Sasahara, M. Ohno, et al., Brain Res. 827 (1999) 130–138.
[13] K. Mishima, S. Higashiyama, A. Asai, K. Yamaoka, et al., Acta Neuropathol. 96 (1998) 322–328.
[14] C.H. Shin, J.P. Robinson, J.A. Sonnen, et al., Oncogene 36 (2017) 4610–4618.
[15] A.S. Ladokhin, A. Kyrychenko, M.V. Rodnin, V. Vasquez-Montes, Methods Enzymol 649 (2021) 341–370.

[16] S.N. Sugiman-Marangos, S.K. Gill, M.J. Mansfield, et al., Commun. Biol. 5 (2022) 375.
[17] T. Mitamura, T. Umata, F. Nakano, et al., J. Biol. Chem. 272 (1997) 27084–27090.
[18] A.E. Arnold, L.J. Smith, G. Beilhartz, et al., Sci. Adv. 6 (2020) eaaz4848.
[19] Y.M. Li, D.A. Vallera, W.A. Hall, J. Neurooncol. 114 (2013) 155–164.
[20] D.W. Laske, R.J. Youle, E.H. Oldfield, Nat. Med. 3 (1997) 1362–1368.
[21] Z. Mohseni, H. Sedighian, R. Halabian, J. Amani, E. Behzadi, A.A. Imani Fooladi, Eur. J. Pharmacol. 899 (2021) 174057.
[22] C. Jordan, K. Siebold, P. Priegue, P.H. Seeberger, R. Gilmour, J. Am. Chem. Soc. 146 (2024) 15366–15375.
[23] G. Tosi, A. Vilella, P. Veratti, et al., Mol. Pharm. 12 (2015) 3672–3684.
[24] E. Rustamzadeh, W.A. Hall, D.A. Todhunter, et al., Int. J. Cancer 120 (2007) 411–419.
[25] D.A. Vallera, C. Li, N. Jin, A. Panoskaltsis-Mortari, W.A. Hall, J. Natl. Cancer Inst. 94 (2002) 597–606.
[26] D.A. Vallera, B.J. Stish, Y. Shu, et al., Gut 57 (2008) 634.
[27] J.S. Brooke, J.H. Cha, L. Eidels, Biochem. Biophys. Res. Commun. 248 (1998) 297–302.
[28] G.V. Louie, W. Yang, M.E. Bowman, S. Choe, Mol. Cell 1 (1997) 67–78.
[29] T. Mitamura, S. Higashiyama, N. Taniguchi, M. Klagsbrun, E. Mekada, J. Biol. Chem. 270 (1995) 1015–1019.
[30] J.M. Rolf, H.M. Gaudin, L. Eidels, J. Biol. Chem. 265 (1990) 7331–7337.
[31] V.M. Richon, Br. J. Cancer 95 (2006) S2–S6.
[32] J.M. Su, L.B. Kilburn, D.B. Mansur, et al., Neuro. Oncol. 24 (2022) 655–664.